[CANCER RESEARCH 63, 4538–4546, August 1, 2003]

Genome-wide Analysis of Gene Expression Associated with *MYCN* in Human Neuroblastoma[1,2]

Miguel Alaminos, Jaume Mora,[3] Nai-Kong V. Cheung, Alex Smith, Jing Qin, Lishi Chen, and William L. Gerald[4]

Departments of Pathology [M. A., L. C., W. L. G.], Pediatrics [J. M., N-K. V. C.], and Epidemiology and Biostatistics [A. S., J. Q.], Memorial Sloan-Kettering Cancer Center, New York, New York 10021

ABSTRACT

Molecular mechanisms through which *MYCN* expression contributes to the malignant phenotype of neuroblastoma are unknown. We performed a genome-wide gene expression analysis of 40 well-characterized neuroblastic tumors and 12 cell lines to identify genes and biological pathways associated with *MYCN* expression. Gene expression was validated by reverse transcription-PCR and immunohistochemistry using tissue arrays. Two hundred twenty-two of 62,839 oligonucleotide probe sets detected expression of genes that were strongly associated with *MYCN* expression. Differentially expressed genes included examples of known oncogenes, genes associated with neural differentiation, and genes related to cell proliferation. Expression of a subset of these genes was altered after transfection of a neuroblastoma cell line, SK-N-ER, with a *MYCN* expressing gene construct when protein synthesis was inhibited and have consensus *MYCN* binding E-box sequences in their promotor regions, suggesting they represent direct targets. Several novel genes/expressed sequences were identified as overexpressed and most likely coamplified with *MYCN* in a subset of cases. A classification model to identify neuroblastomas with high levels of *MYCN* expression was developed based on expression profiles. The identification of coexpressed and coamplified genes associated with *MYCN* overexpression in neuroblastoma suggests biochemical pathways that contribute to the malignant behavior of these tumors and forms a basis for molecular classification.

INTRODUCTION

Neuroblastoma is the most common extracranial malignant solid tumor in infants and children younger than 4 years (1). Prognosis is highly variable and correlates with many biological and clinical features, including age, stage (2), tumor ploidy (3), and other cellular and molecular properties of primary tumors. Outcome remains very poor for stage 4 noninfant patients despite multimodality treatments (4). *MYCN* amplification occurs in ~25% of neuroblastomas and can be detected as homogeneously staining regions or double minutes. The size of the amplicon may vary, and genes adjacent to *MYCN* are frequently amplified (5, 6). Gene amplification is consistently associated with high levels of *MYCN* expression (7). Numerous studies have demonstrated an association between *MYCN* gene amplification and aggressive neuroblastoma (8, 9), however, the molecular mechanisms through which *MYCN* expression governs clinical behavior is unknown (10).

The *MYC* family consists of five genes (11): *MYC* (or *c-myc*); *MYCN*; *MYCL*; *MYCB*; and *MYCS*, with several variants described for *MYCL* (12). All *MYC* genes encode a basic helix-loop-helix leucine zipper protein and are believed to play a role in transcriptional regulation. Two different consensus E-box promoter binding site sequences have been described, CACGTG (13) and CATGTG (14). *MYCN* is believed to primarily serve as a transcriptional activator, although down-regulation of some genes has recently been reported (15, 16).

Overexpression of the MYCN protein is weakly transforming, and this oncogenic role is enhanced by cooperating events such as *RAS* mutation (17). *MYCN* is also thought to have a role in apoptotic cell death under certain conditions (18, 19). Expression of *MYCN* in nonamplified neuroblastoma cell lines can induce reentry of quiescent cells into the cell cycle (20), and a correlation has been shown with growth rate, motility, and cell attachment (21). The most compelling experimental evidence for a critical role of *MYCN* in neuroblastoma is the development of neuroblastoma-like tumors in transgenic mice with neuroectodermal-specific expression of *MYCN* (22). However, the specific targets of this gene remain unknown, and few studies have been performed to investigate in a comprehensive way the function of *MYCN* in human tumors (19, 23, 24). We performed a genome-wide gene expression analysis of well-characterized neuroblastic tumors to identify genes and biological pathways associated with high levels of *MYCN* expression.

MATERIALS AND METHODS

Patient Tumor Samples and Cell Lines. Samples of 40 neuroblastic tumors (Supplemental Table 1) were obtained at the time of surgery and immediately frozen in liquid nitrogen. Three were classified as ganglioneuroma, 3 were stage 4S, 5 stage 2, 8 stage 3, and 21 stage 4. Histological sections of the frozen tissue samples were reviewed, and the areas of interest were manually dissected to provide consistency and avoid nontumoral tissues (>70% tumor cell content). An additional set of 8 neuroblastic tumors (2 ganglioneuromas, 1 stage 2, 1 stage 3, and 4 stage 4 neuroblastomas) were used for validation of the classification algorithm. Twelve neuroblastoma cell lines were also included in the study (Supplemental Table 1; Ref. 25).

Gene Expression Analysis. Total RNA was extracted using Trizol reagent (Life Technologies, Inc., Gaithersburg, MD) and purified with the Qiagen RNeasy System (Qiagen, Mississauga, Ontario, Canada), according to the manufacturers' recommendations. RNA concentration was determined by absorbency at 260 nm, and quality was verified by the integrity of 28S and 18S rRNA after ethidium bromide staining of total RNA samples subjected to 1.2% agarose gel electrophoresis. Total cDNA was synthesized with a T7-polyT primer and reverse transcriptase (Superscript II, Life Technologies, Inc., Carlsbad, CA) before *in vitro* transcription with biotinylated UTP and CTP (Enzo Diagnostics, Farmingdale, NY). Labeled nucleic acid target quality was assessed by test 2 arrays and then hybridized (45°C for 16 h) to Affymetrix Human U95 oligonucleotide arrays. After an automated process of washing and staining, absolute values of expression were calculated and normalized from the scanned array using Affymetrix Microarray Suite 4.0 or 5.0. Gene assignments to probe sets identified as candidate targets of MYCN were identified through the Affymetrix web site[5] and BLAST search of the ENSEMBL human database.

Vectors, Cell Lines, and Transfection Assays. pMYCN (gift of Dr. Naohiko Ikegaki, Fig. 4*A*) contains a 1.6-Kb cDNA fragment corresponding to

Received 1/13/03; accepted 5/14/03.

The costs of publication of this article were defrayed in part by the payment of page charges. This article must therefore be hereby marked *advertisement* in accordance with 18 U.S.C. Section 1734 solely to indicate this fact.

[1] This work was supported, in part, by a research fellowship (to M. A.) from Caja Madrid and the Spanish National Center for Cancer Research, a Career Development Award from American Society of Clinical Oncology (to J. M.), the Translational and Integrative Medicine Research Fund and the Robert Steel Foundation.

[2] Supplementary data for this article are available at *Cancer Research Online* (http://cancerres.aacrjournals.org).

[3] Present address: Department of Hematology and Oncology, Hospital Sant Joan de Deu de Barcelona, Passeig de Sant Joan de Deu num 2, 08950, Esplugues del Llobregat, Barcelona, Spain.

[4] To whom requests for reprints should be addressed, at Department of Pathology, Memorial Sloan-Kettering Cancer Center, 1275 York Avenue, New York, NY 10021. Phone: (212) 639-5858; Fax: (212) 639-4559.

[5] Internet address: http://www.affymetrix.com/index.affx.

exons 2 and 3 of the *MYCN* gene under control of a *CMV* immediate early promoter. For transfection, cell lines were grown in RPMI culture medium (SK-N-ER neuroblastoma cell line) or Dulbecco's modified Eagles high glucose culture medium (SK-N-AS and COS-1 cells) with 10% FCS at 37°C to near confluence. Cells (10^6) were transfected with 2 μg of the plasmid (pMYCN or pCMV6) with Lipofectamine (Life Technologies, Inc.) and incubated for 24 h in the absence of serum during the first 12 h. Cells were harvested in the cold and protein lysates prepared by addition of lysis buffer [1% NP40, 150 mM NaCl, 50 mM Tris HCl (pH 8), and 2 mM phenylmethylsulfonyl fluoride]. For some transfections, cycloheximide (20 μg/ml) was added to the culture medium 20 min before transfection and for 24 h (26). Total RNA was extracted using Trizol reagent. Protein concentration was determined by Bio-Rad D_C protein assay system (Bio-Rad Laboratories, Hercules, CA).

SDS-PAGE Gel Electrophoresis and Western Blot. A total of 25 μg of each total cell protein extract was loaded on Nu-PAGE polyacrylamide gels (Invitrogen Corporation, Carlsbad, CA), separated by electrophoresis, and transferred to nitrocellulose membranes according to standard procedures. Incubation with anti-MYCN antibody (Oncogene Research, Darmstadt, Germany) and anti-β-tubulin antibody (Sigma-Aldrich Corp., St. Louis, MO) was carried out for 1 h at a dilution of 1:250, followed by hybridization to secondary antibody for 1 h. Anti-RAN antibody (Santa Cruz Biotechnology, Santa Cruz, CA) was used at a dilution of 1:500.

cDNA Southern Blotting. Total cDNA was synthesized from 1 μg of RNA by using the SMART PCR cDNA synthesis kit (Clontech Laboratories, Palo Alto, CA) and amplified by 17 PCR cycles to avoid overamplification of the more abundant cDNA fragments (this number was determined by agarose gel analysis of PCR products after each new cycle). Amplified total cDNA fragments were separated by agarose gel electrophoresis and transferred to a nylon membrane. *MYCN* probe was prepared by PCR amplification of the insert in pMYCN with digoxigenin-labeled deoxynucleotide triphosphates. Hybridization was carried out overnight at 42°C in a 50% formamide buffer.

Real-Time RT-PCR. Real time RT-PCR[6] was carried out with 100 ng of each total RNA template and 18 μl of a master mix prepared according to the manufacturer (LightCycler Master Kit; Roche, Basel, Switzerland). All reactions were performed in the LightCycler thermocycler with water in place of template as a negative control and a specific RNA used as a positive control. MYCN primers were 5′-CTCAGTACCTCCGGAGAG-3′ and 5′-GGCATCGTTTGAGGATC-3′.

Data Analysis. Absolute values of expression for the *MYCN* gene (based on hybridization to the 35158_at probe set) were used to classify the samples as those with a high level of *MYCN* expression (>10,000) or low level (<10,000). This cut point was established as described in results below. This probe was also used as an independent variable for the correlation test. Because the gene expression data were skewed such that normality assumptions for parametric tests were not met, we used the Mann-Whitney test that uses rank statistics. To take both magnitude and rank into account, we have used the following two-step approach to identify differentially expressed genes: (*a*) fold change was calculated as a ratio of the means of both comparison groups (*MYCN* expressers *versus* nonexpressers). To avoid placing emphasis on genes where overall expression was low across all samples, a minimum expression threshold was established, and any expression mean observed to be <200 was automatically set to 200. (*b*) *P* was determined by Mann-Whitney and Kendall's *tau* tests for all genes. *P* based on either of these two nonparametric tests was calculated. Both are rank-based and, thus, ignore the magnitude of the expressions values. Although the *P*s from either of these tests serve as a convenient mechanism to draw an additional cutoff on genes of interest or to rank the genes, we did not rely on them for inferring statistical significance. It is likely that conducting thousands of simultaneous tests for all genes on gene chips could magnify the false discovery rate.

Datasets used for hierarchical clustering were normalized by standardizing each expression level of each gene and each sample to mean = 0 and variance = 1.

Gene filtering, hierarchical clustering, and result display were performed using Cluster and Tree-View (Stanford University, Palo Alto, CA).

Development of Classification Models. A stepwise logistic regression approach was used to identify the subset of genes providing the most accurate classification of samples. First, a univariate logistic regression model with a response of high *versus* low *MYCN* expression was fit for each of the genes that satisfied all filter requirements. Any probe sets corresponding to *MYCN* or potentially coamplified genes were excluded from candidacy. The probe set having the smallest AIC was selected as the single best classifier (27). After selecting this probe set, logistic regression models were again fit for each gene or expressed sequence in conjunction with the previously selected probe set in the model. The gene providing the smallest AIC (*i.e.*, the maximum decrease in AIC after inclusion of the first probe set) was selected as the second best gene. This procedure was repeated until no additional reduction in AIC was observed by the inclusion of additional genes into the model.

Immunohistochemistry, Immunocytochemistry, and Immunofluorescence. Multitissue blocks of formalin-fixed, paraffin-embedded tissues corresponding to the samples used in this study were prepared by using a tissue arrayer (Beecher Instruments, Silver Spring, MD). The blocks contained three representative 0.6-mm cores from diagnostic areas of each case and control tissue. Immunohistochemical analysis of tissue sections and cell lines grown directly on slides was carried out with standard streptavidin-biotin peroxidase methodology using microwave antigen retrieval and anti-MYCN antibody (Oncogene Research, Darmstadt, Germany) 1:100. As negative controls, we used SK-N-ER cell lines (a well described non-*MYCN*-amplified neuroblastoma cell line with very low levels of expression of this gene) as well as normal kidney and normal adrenal medulla. As a positive control, the same cell line was used after transfection with a *MYCN* gene expression construct, along with the previously described *MYCN*-amplified cell line LAN-1 with constitutively high levels of expression of *MYCN*.

FISH. Bicolor FISH was performed on touch imprints obtained from frozen tumor samples using commercially available probes for *MYCN* and chromosome 17 centromere-specific alphoid region (Vysis, Downer's Grove, IL), according to standard protocols (28). The number of hybridization signals for each probe was assessed in a minimum of 200 interphase nuclei with strong and well-delineated signals. As controls, normal peripheral blood lymphocytes were simultaneously hybridized. Samples were considered *MYCN* amplified when >10 copies of the gene are found in >90% of the cells.

RESULTS

Relationship of *MYCN* RNA Levels to Gene Copy Number and Intranuclear Protein Expression. Genome-wide gene expression analysis was performed for 40 neuroblastic tumors and 12 neuroblastoma cell lines using oligonucleotide arrays with 62,839 probe sets (Supplemental Table 1). Relatively high levels of *MYCN* mRNA were detected in nine of nine *MYCN*-amplified cell lines and seven of nine *MYCN*-amplified tumor samples (Fig. 1*A*). In addition, 4 nonamplified tumor samples had high levels of this mRNA. Validation of *MYCN* RNA levels was carried out for some samples using LightCycler real-time PCR, and a good correlation with microarray-determined RNA levels was found (Fig. 1*B*). *MYCN* gene copy number/cell was confirmed by interphase locus-specific FISH in all six cases for which gene copy number and level of expression were discordant (Fig. 2, *A* and *B*). The presence of MYCN protein was determined by immunohistochemistry and immunofluorescence in tumors for which material was available. Nine of 10 tumors (90%) expressing high levels of *MYCN* mRNA were immunoreactive for nuclear MYCN protein by immunohistochemistry and immunofluorescence (Figs. 1*A* and 2, *C* and *D*). One tumor with high levels of *MYCN* mRNA (no. 55) did not demonstrate the presence of MYCN protein with either technique, and 1 of 21 tumors with low mRNA level (no. 36) was weakly immunoreactive for nuclear MYCN protein. Most samples with *MYCN* gene amplification and protein expression have *MYCN* RNA levels above an inflection between samples NE-NA/2/12 (8,000 FU) and the amplified cell line sample E-A/SK-N-JD (36,000 FU). We therefore decided to use a cut point near this inflection that would separate tumors with both amplification and high relative levels of expression from the remaining samples. Samples with expression above 10,000 FU were defined as having high levels of *MYCN* (11

[6] The abbreviations used are: RT-PCR, reverse transcription-PCR; AIC, Akaike Information Criteria; FISH, fluorescent *in situ* hybridization; FU, fluorescent unit.

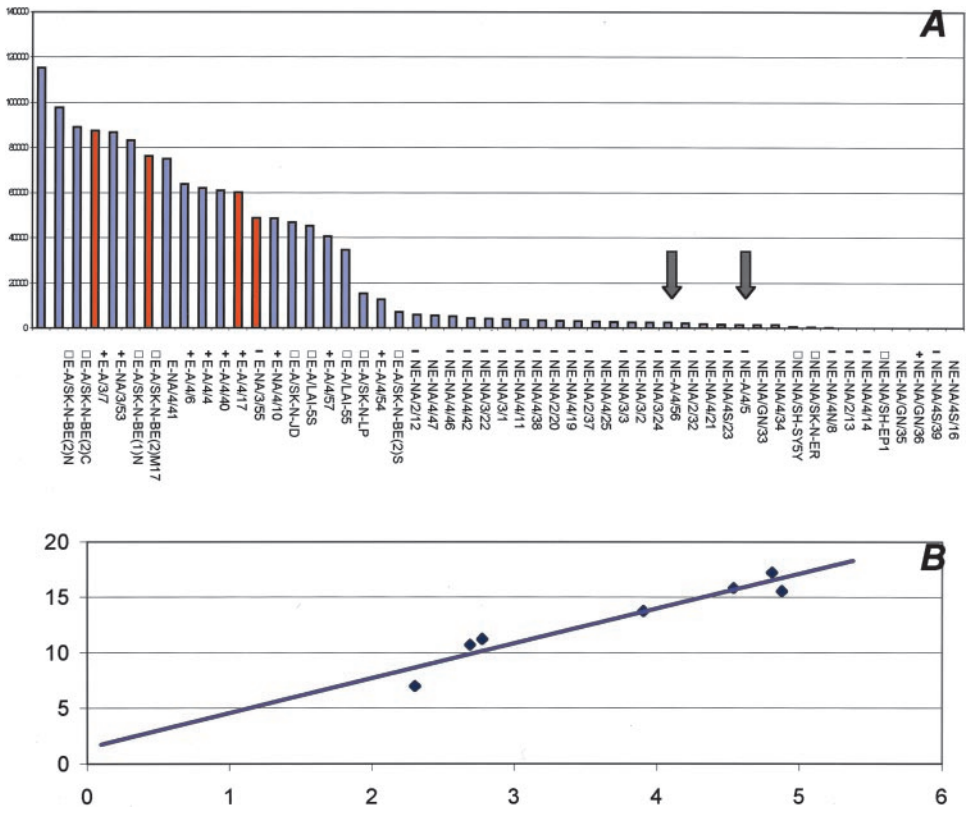

Fig. 1. *A*, histogram of *MYCN* expression across all samples. A: *MYCN*-amplified tumors and cell lines; NA: nonamplified; E: samples with high levels of *MYCN* expression; NE: samples with low level *MYCN* expression. The International Neuroblastoma Staging System stage for each case precedes its tumor identification number. The *arrows* indicate the two cases with *MYCN* amplification that do not express *MYCN* RNA. Detection of nuclear MYCN by immunohistochemistry in the sample is indicated along with the sample identifier (+ indicates protein expression; − is negative; ▲ means that those cell lines were previously characterized by Western blot (25); and blanks are nonavailable data). *B*, plot of microarray-determined MYCN transcript level (logarithm of the absolute expression value determined by microarray analysis, in *X* axis) *versus* MYCN RNA levels determined by quantitative RT-PCR (expressed in LightCycler fluorescent units in the *Y* axis).

tumor samples and 9 cell lines) for the purposes of comparison to samples with low level *MYCN* expression (29 tumors and 3 cell lines).

Identification of Genes with Expression Patterns that Correlate with *MYCN*. Unsupervised, average-linkage, hierarchical cluster analysis of all tumor samples using ~7000 probe sets with the greatest variance (based on the difference between the maximum value and minimum value of at least 3000 FU) demonstrated that samples with high levels of *MYCN* expression have expression profiles that tended to correlate more strongly with each other than with tumors having low levels of *MYCN* expression (Fig. 3*A*). Nine of 11 *MYCN*-expressing tumors were grouped on the same tertiary node of the dendrogram. However, it should be noted that this observation is based on a

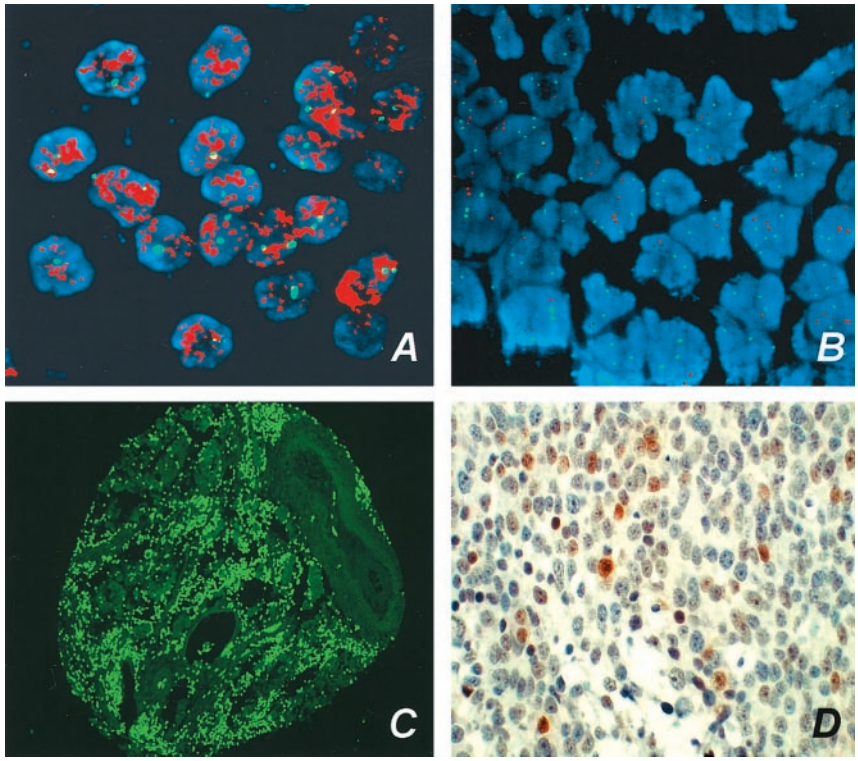

Fig. 2. *A*, photomicrograph of the FISH assay for a *MYCN*-amplified, nonexpressing tumor (case no. 56). *B*, non-*MYCN*-amplified sample with high levels of *MYCN* expression (case no. 53). *Red signals* represent the *MYCN*-specific probe. *Green* represents the chromosome 17 centromeric probe used as a control of ploidy. *C*, immunofluorescence (×40 magnification) assay for MYCN protein in a positive case (sample no. 4). *D*, immunohistochemistry (×200 magnification) for the same protein in the same case.

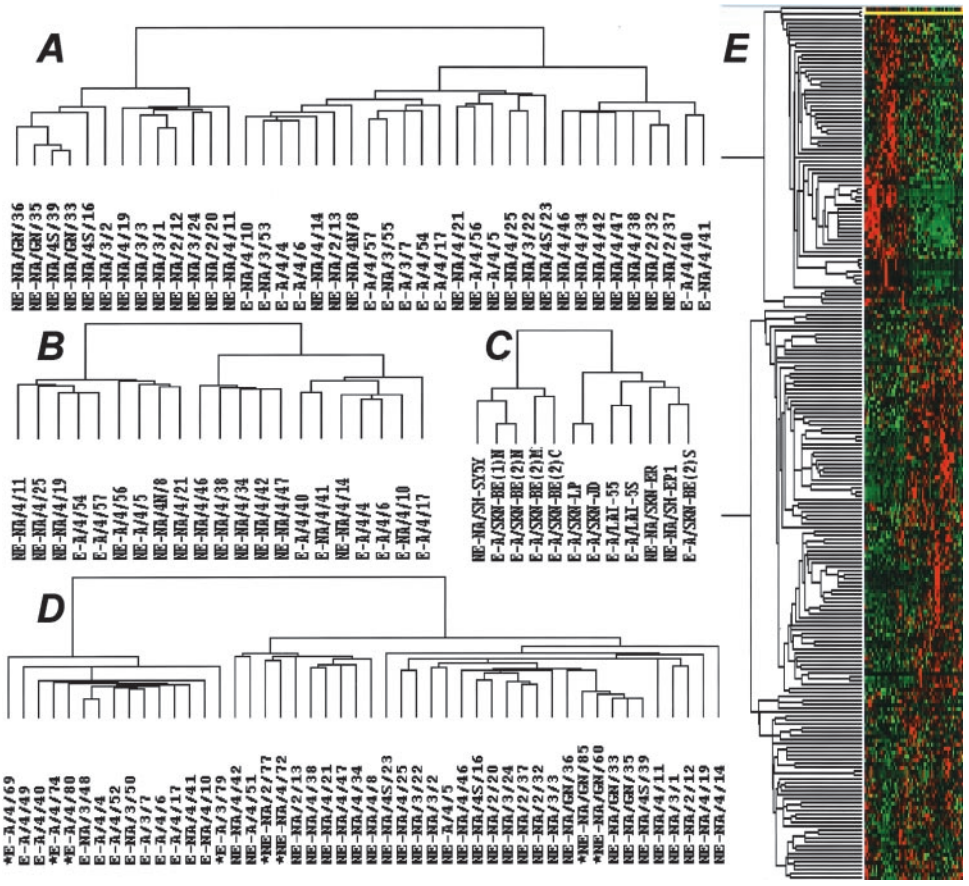

Fig. 3. *A*, dendrogram representing cluster analysis of all neuroblastic tumors. The analysis was performed for all probe sets after filtering to prevent noise derived from probe sets with no differential expression along the samples set. A: *MYCN*-amplified tumors and cell lines; NA: nonamplified; E: samples with high levels of *MYCN* expression; NE: samples with low level *MYCN* expression. The International Neuroblastoma Staging System stage of each case precedes tumor identification number. The same approach was used for stage 4 tumors only (*B*) and neuroblastoma cell lines only (*C*). *D*, cluster of all neuroblastic tumors (training and test samples with test samples indicated by an *asterisk*) demonstrating the strong differential expression of the 222 probe sets having significant correlation with *MYCN*. *E*, cluster tree representation of the 222 probe sets in the analysis of all neuroblastic tumors.

relatively small sample size, and this correlation was less evident when only stroma poor, stage 4 tumors were included in the analysis (Fig. 3*B*) and for neuroblastoma cell lines (Fig. 3*C*).

To identify genes with expression that correlated with *MYCN* levels, we compared tumors with and without high levels of *MYCN* mRNA as defined above. We used three statistical and mathematical measures to select probe sets with significant, large, relative expression differences between the two groups. Absolute values of expression for every probe set and every tumor sample were compared with that of a representative *MYCN* gene probe set (U95A 35158_at) using the Kendall *tau* test to select for those genes with expression patterns that were strongly correlated with *MYCN*. To detect genes with significant relative quantitative differences in the expression values between tumors with high- and low-level of *MYCN* mRNA, we used a Mann-Whitney nonparametric test and set a threshold of at least a 3-fold difference. Two hundred twenty-two of 62,839 probe sets met all three criteria (Kendall *tau* correlation and Mann-Whitney tests $P < 0.01$ and at least a 3-fold-change in mean expression; Supplemental Table S2). Seventy-four probe sets detected genes that were up-regulated and 148 that were down-regulated in tumors with high levels of *MYCN* RNA.

We assigned a general biological function to all characterized genes that correlated with *MYCN* based on the Gene Ontology web site and literature review. Although a large proportion were of unknown function (63.9%), a number of genes were related to cell proliferation and neural differentiation. Fifteen of 80 partially characterized genes are thought to play a role in neural differentiation or neuronal function and 12 of 15 were down-regulated in tumors with high levels of *MYCN*. Four *MYCN*-associated genes were related to cell cycle regulation or cell proliferation. These findings correlate well with the lack of differentiation and high mitotic-karyorrhectic index that is common for *MYCN*-amplified tumors, especially in younger patients (29).

Because most neuroblastomas with *MYCN* amplification are poorly differentiated and high stage, we performed the same analysis comparing 8 tumors with high levels of *MYCN* expression and 13 tumors with low levels of *MYCN* expression that were matched for stroma poor histology and stage 4 disease. Seventy-nine probe sets met the strict criteria of $P < 0.01$ for both Mann-Whitney and Kendall tests and 3-fold-change mean expression (Supplemental Table S3). Twenty-two of these probe sets (27.8%) were also identified as differentially expressed in the analysis of all neuroblastic tumors. Of the 79 genes differentially expressed with *MYCN* in stroma poor stage 4 tumors, we were able to assign a general biological function for 43. Three encoded DNA binding or DNA-associated proteins (NR5A1, CRE-Bpa, and H1F5) that are overexpressed with *MYCN* expression, as well as the oncogenes *KIT* and *TGFBI* [encoding a protein induced by transforming growth factor β (30)]. Two cell adhesion-related genes (occludin and protocadherin β4) were significantly overexpressed in tumors with low levels of *MYCN*. Down-regulation in *MYCN* tumors of two genes implicated in development and histogenesis (*HPX-42* and *SIX6*) supports the role of *MYCN* in primitive cell populations. On the other hand, the genes *CDCA7* and *LOC166867*, both with a function of control of the cell cycle and the mitotic spindle checkpoint, are overexpressed in tumors with high levels of *MYCN*, most likely reflecting the high mitotic rate found in these tumors, whereas FGF9 (one of the genes controlling neural cell proliferation) was down-regulated. The 22 genes that were consistently differentially expressed in comparisons of all tumors and comparisons of stage 4 tumors were mostly uncharacterized, although genes encoding histone H4, synaptic vesicle membrane protein VAT, and the *MYC* target gene *CDCA7* were included, along with three genes that are

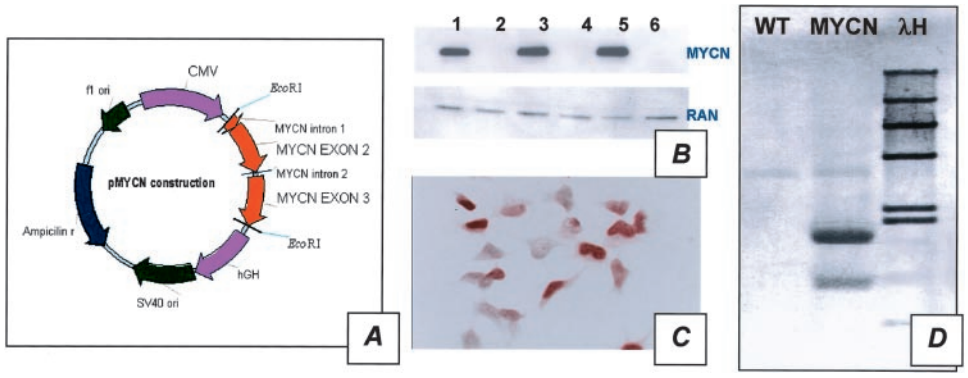

Fig. 4. *A*, schematic representation of the pMYCN. *B*, Western blot for the MYCN protein and the control protein RAN. *Lane 1:* SK-N-ER cells transfected with pMYCN; *Lane 2:* SK-N-ER transfected with pCMV6; *Lane 3:* SK-N-AS transfected with pMYCN; *Lane 4:* SK-N-AS transfected with pCMV6; *Lane 5:* COS-1 transfected with pMYCN; *Lane 6:* COS-1 transfected with pCMV6. *C*, immunocytochemistry on adherent SK-N-ER cells with the anti-MYCN antibody shows strong nuclear positivity of transfected cells. *D*, cDNA Southern blotting assay for SK-N-ER cells before (WT) and after transfection with the plasmid pMYCN (MYCN). λH is λ phage DNA digested with *Hin*dIII as size marker.

commonly coamplified with *MYCN* (*DDX1*, *NCYM*, and *NAG*; Supplemental Tables 2 and 3). Many of the genes associated with neural differentiation and proliferation rate that were identified as differentially expressed in *MYCN*-related tumors when compared with all others were not as strongly differentially expressed when tumors were matched for histology and stage. These results are not surprising because aggressive tumors are expected to have similar biological attributes regardless of *MYCN* status.

MYCN Regulation of Gene Expression in Transfected Cell Lines. *MYCN* is believed to function as a DNA binding transcription factor. Therefore, it is likely that some of the gene expression differences we detected in neuroblastic tumors with high levels of *MYCN* expression are attributable to direct regulation by *MYCN*; others may be downstream effects or indirect consequences. We used *MYCN* transfection of neuroblastoma cell lines with low level expression of *MYCN* to identify early events and direct gene targets. The pMYCN-transfected cell lines demonstrated strong expression of *MYCN* mRNA by cDNA Southern blotting (Fig. 4*D*), and MYCN protein was detected by Western blot (Fig. 4*B*) and immunocytochemistry (Fig. 4*C*). Strong nuclear immunoreactivity for MYCN was detected in ~15–20% of cells in the pMYCN-transfected cultures and reflects the transfection efficiency. To identify those genes that might be direct targets, we transfected SK-N-ER cells with pMYCN in the presence of cycloheximide and performed expression analysis to identify those genes that are differentially expressed. Under the experimental conditions, MYCN protein is synthesized albeit at a reduced level and protein synthesis is largely inhibited over the 24-h period of incubation. Seventy-three of 222 probe sets identified as differentially expressed in tumor samples also exhibited qualitatively similar changes (>10% increase or decrease) after *MYCN* transfection in the presence of cycloheximide. Thirty-nine of these exhibited a >50% change and 26 a >100% change. Because only ~20% of cells are transfected, even small changes may be meaningful, but the greater the change the more likely that it is a reproducible (Supplemental Table S2). Regulation in the presence of a protein synthesis inhibitor suggests that these genes could be direct targets of *MYCN*. As additional support for putative direct interaction by *MYCN*, we analyzed the DNA sequences corresponding to potential promoter regions of the 222 differentially expressed genes. Four thousand-bp 5′ to the ATG start codon for 139 differentially expressed genes with available sequence were searched for the consensus E-box sequences recognized by *MYCN*, CACGTG, and CATGTG (14).[7] A consensus binding motif was detected in 110 (79.1%) regions (CACGTG in 41 genes and CATGTG in 95 genes). This frequency was significantly higher than that found in a parallel analysis of the putative promoter regions of 100 randomly selected genes that were not on the list of 222 (χ^2 test yielded P of 0.0002). Fifteen of 39 probe sets differentially expressed in tumor samples (>50%) after transfection of SK-N-ER with cycloheximide, and with available sequence, contained an E-box sequence within the 5′ untranslated sequence.

Cell Context Specificity of *MYCN* Function. Physiological gene regulation by *MYCN* is cell context dependent and requires the presence of cooperating molecules and chromatin structure. These features are expected to vary from cell to cell and within the spectrum of human tumors (20). To gain an understanding of the influence of cell context and to identify *MYCN*-regulated genes that are not dependent on cellular milieu, we analyzed gene expression in two separate neuroblastoma cells lines that were shown to have low levels of *MYCN* expression (SK-N-ER, SK-N-AS) along with COS-1 cells. Labeled targets from each cell line 24 h after transfection with either the pMYCN construct or control pCMV6 were hybridized to oligonucleotide arrays. Each transfected cell line demonstrated a relatively cell-specific pattern of differential gene expression with only 12.2% of all probe sets demonstrating the same direction of change (>10% increase or decrease) in expression after *MYCN* transfection in all three lines. These results suggest that there is a strong cell context influence on *MYCN* activity with a relatively small number of consistent changes in gene expression identified.

Of the 222 probe sets detecting significant association with *MYCN* expression for tumors, 29 showed similar directional changes in both neuroblastoma cell lines (SK-N-ER and SK-N-AS cells) with transfection (Supplemental Table S2). Thirteen of 29 genes showed the same directional changes in presence of cycloheximide.

Expressed Genes in the *MYCN* Amplicon. In an effort to identify differentially expressed genes that may be part of the *MYCN* amplicon, we examined all genes and ESTs reported to map to chromosome 2 with expression patterns that strongly correlated ($P < 0.01$ for Kendall *tau* correlation test) with *MYCN*, *DDX1*, and *NAG* expression, genes that are often part of the *MYCN* amplicon. The results suggest that several adjacent genes that have not previously been implicated in *MYCN* amplification (*RPS7*, *ACP1*, *GREB1*, *MGC11266*, *DKFZP566A1524*, *NSE1*, and the uncharacterized gene Hs.110039) are overexpressed and potentially coamplified in some neuroblastomas. An expression map of the region corresponding to neuroblastomas with high levels of *MYCN* expression (Fig. 5) demonstrates that *MYCN* is the only gene consistently expressed in all neuroblastomas with 2p amplification and agrees with the findings of others (6, 31). The significance of overexpression of coamplified genes is unknown.

Molecular Classification of Neuroblastoma. We evaluated the 222 genes that passed all filters in an attempt to develop a method for classification of neuroblastoma according to *MYCN* status. Such a classification would be useful in the case of discordant tumors or neuroblastomas that have alterations in MYCN regulated pathways independent of alterations in MYCN status, although it is

[7] Internet address: http://genome.ucsc.edu/cgi-bin/hgGateway.

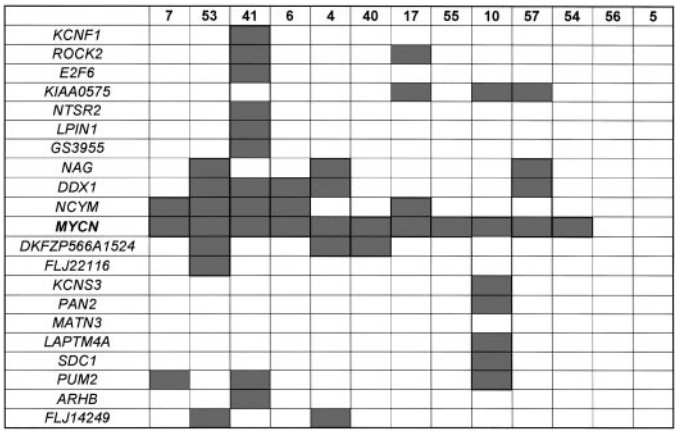

Fig. 5. Expression of genes near *MYCN* in samples showing amplification or overexpression of this gene. Map is derived from the University of California Santa Cruz genome database.[7] indicates expression at least one SD above the mean for that gene in tumor samples.

uncertain such tumors exist. In addition MYCN-independent classification methods may supplement standard gene copy assays to provide greater diagnostic confidence. Six genes were excluded from model development because they were likely associated with *MYCN* amplification. A stepwise logistic procedure using the remaining 216 candidate probe sets and the 40 training tumor samples (29 high and 11 low *MYCN* expressers) was used to identify a number of two-gene models that were equally sufficient in leading to perfect group separation of all 40 samples. One probe set (44577_at corresponding to a partially characterized gene) was the dominant first choice in a model because it univariately led to correct classification of 38 of 40 samples. When each of the remaining genes was examined alongside this first choice in a two-gene classification model, it was found that 111 different choices of second probe sets all led to perfect classification of the training samples. We considered each of these models in classifying a validation set of eight additional test samples (Supplemental Table 1), five high and three low *MYCN*, to compare prediction accuracy. Of the 111 potential models, 92 led to perfect eight of eight classification, 14 led to seven of eight, and only 5 led to six of eight. This is highly encouraging that these results will continue to prove reproducible in the classification of future samples. One of the models that led to perfect classification of the validation set of samples was selected (Fig. 6) and an algorithm to predict *MYCN* status based in these two probe sets [44577_at and 37173_at (centrosome associated protein E)] is proposed: $P = 1 / [1 + e^{(188.5 - 0.035X_1 + 0.065X_2)}]$; where P is the probability of a sample to be high *MYCN* expressor and X_1 and X_2 represent the raw expression value of probe sets 44577_at and 37173_at, respectively. When classifying future samples, the specific values of X_1 and X_2 of the test samples could be input into the equation and the estimated probability could then be used to classify the sample as high *MYCN* ($P > 0.5$) or low *MYCN* ($P < 0.5$). Additional support to the validity of this algorithm comes from the fact that the status of *MYCN* was correctly predicted in 12 of 12 neuroblastoma cell lines tested (Supplemental Table 1).

DISCUSSION

MYCN amplification is a well-established clinical marker of aggressive neuroblastoma useful for patient risk stratification. Amplification leads to high levels of gene expression in the majority of cases, and it is assumed that increased *MYCN* levels contribute directly to tumor biology. *MYCN* is a transcriptional regulator, however, few specific *in vivo* targets have been identified and the mechanisms by which *MYCN* contributes to aggressive tumor biology are not known. We used oligonucleotide arrays with >62,000 probe sets to monitor the effects of *MYCN* in neuroblastoma through analysis of human tumors and cell lines and identified a number of candidate genes that may represent direct and indirect targets of this oncogene. An interesting finding from our analysis that has also been noted in previous studies (8, 32, 33) is that *MYCN* mRNA expression levels did not always coincide with *MYCN* gene copy number (10, 34). This implies that overexpression of *MYCN* occurs in some cases of neuroblastoma without gene amplification and is probably attributable to alterations in transcriptional regulation of *MYCN*, although other possibilities exist (35). The clinical significance of overexpression in the absence of amplification is uncertain. However, in this study, tumors with high levels of *MYCN* expression in the absence of amplification tended to cluster with amplified tumors with increased expression, demonstrating a correlation between level of *MYCN* expression and overall gene expression profile.

It is believed that *MYCN* is able to trigger diverse complex pathways that may contribute to tumor biology, but the exact nature of these pathways has not been clarified. It may be that *MYCN* acts as a master transcriptional regulator controlling other genes that more directly activate or repress critical biological pathways. In fact, some transcriptional regulators (*HTATIP*, *HTATIP2*, *DDX1*, *MI-ER1*, and *NCYM*) and oncogenes (*NCYM* and *RAB20*) were found in our study to correlate with the status of expression of *MYCN* in neuroblastoma. Two transcriptional activators with histone acetylase activity (*HTATIP* and *HTATIP2*) were down-regulated in *MYCN*-expressing tumors, and the loss of these genes may contribute to resistance to death-inducing signals and is also implicated in small cell lung carcinoma (36, 37). The oncogenes *NCYM* [capable of transforming cells in culture (38)] and *RAB20* [a positive regulator of *RAS* (39)] were overexpressed in *MYCN*-expressing tumors and could contribute to tumor biology.

Many of the genes that are differentially expressed in neuroblastomas with high levels of *MYCN* are involved in development or neural differentiation, suggesting that overexpression of *MYCN* is associated with altered maturation in progenitor neuroectodermal

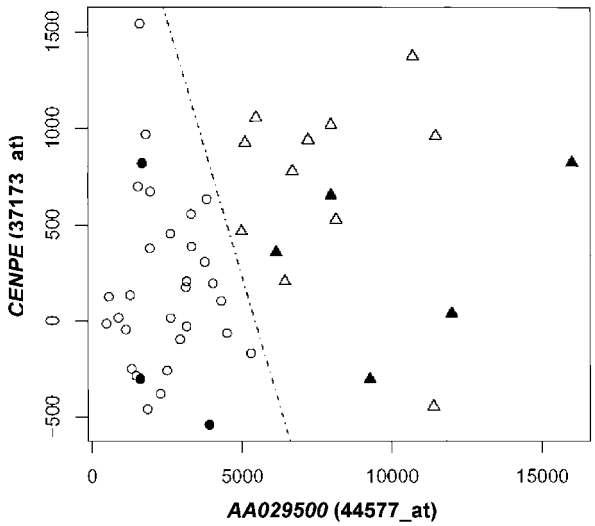

Fig. 6. Plot of individual samples demonstrating logistic regression classification. The hollow symbols (○ and △) represent the 40 training samples and the solid symbols (● and ▲) represent the 8 test samples. *Triangles* are samples with high *MYCN* expression, and *circles* are non-*MYCN*-expressing tumors.

cells. For example, *HOXC10*, a homeobox gene down-regulated in tumors with high levels of *MYCN*, is normally expressed at high levels in embryonic spinal cord and brain (40, 41), and it is believed to play an important role in development. Homeobox genes may exert a wide spectrum of effects in a variety of organs and body parts during early mammalian development (40). Additional support to the role of *MYCN* in differentiation comes from the fact that many markers of neural differentiation (*PTN*, *FMNL*, *DNER*, *CLU*, *GDA*, *NRCAM*, *ECEL1*, and *SNPH*) were increased in tumors with low *MYCN* levels, consistent with a greater degree of maturation for these tumors. Peripheral myelin protein 22, a marker of Schwann cells (42), and the product of the gene *EMP2* that shares 43% amino acid identity with peripheral myelin protein 22 (43) were down-regulated in *MYCN*-expressing tumors and reflects the stroma poor histology. Two other genes also related to differentiation, *CD44* (44) and the receptor LR8 (45), were more highly expressed in tumors without *MYCN*. Inverse correlation between *CD44* expression and *MYCN* amplification has been reported previously (44). On the other hand, *CASPR3* with a potential role in cell recognition within the nervous system (46), *STAF65*γ [expressed in the brain (47)], and *UNC5C* [related to cerebellar development (48)] were more abundant in *MYCN*-expressing tumors. The differential expression of these genes apparently reflects the primitive cell populations in untreated *MYCN*-amplified tumors.

Some differentially expressed genes are associated with regulation of cell cycle, cell proliferation, and apoptosis. *CDCA7* encodes for a cell division cycle-associated protein with neoplastic potential that has been previously identified as a target of *MYC* (49). *CENPE* has recently been identified as a target of *MYCN* (50) and is significantly up-regulated in *MYCN*-expressing tumors, reflecting the increased proliferation rate present in these tumors. In the same way, *CDC2L2* was found to be up-regulated in tumors with *MYCN* expression, and a role of this cyclin-encoding gene in cell cycle progression has been proposed (51). Of interest, this gene maps at 1p36.3, a region frequently deleted in *MYCN*-amplified tumors (52, 53), and it has been considered a candidate tumor suppressor in neuroblastoma. On the other hand, *PCTAIRE2BP*, a molecule associated with a CDC2-like kinase that is expressed in terminally differentiated neurons (54), was down-regulated in *MYCN*-expressing tumors. Other DNA synthesis and repair-related genes were also up-regulated in tumors expressing *MYCN*, possibly as a consequence of the increased cell proliferation found in these tumors. One of these genes is *UBL1*, encoding for sentrin (55), which has been implicated in regulation of human homologous DNA recombination (56), and another one is *NSE1*, with a function in DNA repair and structural maintenance of chromosomes (57). Several RNAs encoding for proteins that are related to apoptosis and cell death were differentially expressed: *EMP2* (58), *TEGT* (59), and *SST* (60) were more abundant in tumors with low level of *MYCN*, and *BID* was up-regulated. Altered regulation of apoptotic activity may be a key feature of *MYCN*-induced tumorigenesis.

It is interesting that the gene expression distinctions identified through comparisons of neuroblastomas without regard for stage or histology are not as evident when cases for comparison are controlled for these factors. For example, none of the genes related to neural differentiation showed a strong correlation with *MYCN* in stage 4 stroma poor tumors, suggesting that non-*MYCN*-expressing tumors have a similar phenotype to *MYCN*-overexpressing tumors of the same stage.

Although some of the genes identified in this study have been previously associated with *MYCN* [clusterin, *CENPE* (50), *DDX1* (5, 6), *NAG* (6)] or to the oncogene *MYC* [*TUBA1* (25), *CDCA7* (49)], other previously characterized targets of *MYCN* did not meet the stringent criteria used here. For example, 40 probe sets encoding ribosome associated proteins (*RPS3A*, *RPL18A*, *RPL9*, *RPS5*, and others) and other genes [*PTMA* (23), *NCL* (61), *NPM1* (61), and *NME1*(62)] that have been associated with *MYCN* expression in cell lines (61) were not selected in this study because of the requirement for a minimum of 3-fold change, although they demonstrated a statistical correlation with *MYCN* ($P < 0.01$ for Kendall *tau* and Mann-Whitney tests). Different technical platforms could also be a reason for discrepancies. In addition, data from our transfection experiments suggest that cell context could have a dramatic effect on *MYCN* function. The biological differences between cell and tumor samples could explain the apparent variation in differential expression among experiments.

An important aspect of our study was the identification of genes that are likely to be direct targets of *MYCN* regulation based on several lines of evidence, including changes in gene expression after *MYCN* transfection in the presence of cycloheximide, a relationship to *MYCN* overexpression in human tumors, and the presence of a binding site for the MYCN protein within a potential promoter region. Of the 15 probe sets that met all these criteria, *PMP22* is related to neural function and differentiation, *FADS3* has been implicated in the synthesis of membrane fatty acids, *NUMA1* is part of the nuclear mitotic apparatus, and *DBY* encodes for a RNA helicase. Additional characterization of the remaining genes and their transcriptional regulation will help define a direct role of *MYCN* in tumorigenesis.

The *MYCN* amplicon often includes other genes that are overexpressed. One unresolved issue has been to define those genes that are expressed because of coamplification with *MYCN* and may contribute to the biology of neuroblastomas with 2p amplification. We identified seven genes near *MYCN* that were strongly overexpressed in a subset of neuroblastomas with high levels of *MYCN*, some of which had not been previously identified in the *MYCN* amplicon. However, no other gene was found to be highly expressed in every case of neuroblastoma with high levels of *MYCN*, and none was consistently highly expressed in the absence of *MYCN* expression.

With the information derived from these studies, we were able to develop methods of molecular classification that use gene expression profiles to identify neuroblastic tumors with high *MYCN* status. Although these models require independent validation further than the 8 tumors and 12 cell lines samples used in this work, they serve as proof of principle for a clinically relevant molecular subclassification based on gene expression. Defining the molecular profiles of other categories of this heterogeneous disease has a high likelihood of additionally improving our understanding of this enigmatic cancer to refine risk-based therapeutic approaches.

ACKNOWLEDGMENTS

We thank Dr. Naohiko Ikegaki of Children's Hospital of Philadelphia for the pMYCN plasmid, Kevin Cheung for BLAST searches, Sandra Levcovici, and Muzaffar Akram for their technical support. We also thank Shirley Tung for her editorial assistance in the preparation of this article.

REFERENCES

1. Castleberry, R. P. Neuroblastoma. Eur. J. Cancer, *33:* 1430–1437, 1997.
2. Brodeur, G. M., and Maris, J. M. Neuroblastoma. *In:* P. A. Pizzo and D. G. Poplack (eds.), Principles and Practice of Pediatric Oncology, J. B. Lippincott Company, Philadelphia, pp. 895, 2002.
3. Look, A. T., Hayes, F. A., Shuster, J. J., Douglass, E. C., Castleberry, R. P., Bowman, L. C., Smith, E. I., and Brodeur, G. M. Clinical relevance of tumor cell ploidy and *N-myc* gene amplification in childhood neuroblastoma: a Pediatric Oncology Group study. J. Clin. Oncol., *9:* 581–591, 1991.

4. Matthay, K. K. *MYCN* expression in neuroblastoma: a mixed message? J. Clin. Oncol., *18:* 3591–3594, 2000.
5. Amler, L. C., Schurmann, J., and Schwab, M. The *DDX1* gene maps within 400 kbp 5′ to *MYCN* and is frequently coamplified in human neuroblastoma. Genes Chromosomes Cancer, *15:* 134–137, 1996.
6. George, R. E., Kenyon, R. M., McGuckin, A. G., Malcolm, A. J., Pearson, A. D., and Lunec, J. Investigation of co-amplification of the candidate genes ornithine decarboxylase, ribonucleotide reductase, syndecan-1 and a DEAD box gene, DDX1, with *N-myc* in neuroblastoma. United Kingdom Children's Cancer Study Group. Oncogene, *12:* 1583–1587, 1996.
7. Bordow, S. B., Norris, M. D., Haber, P. S., Marshall, G. M., and Haber, M. Prognostic significance of *MYCN* oncogene expression in childhood neuroblastoma. J. Clin. Oncol., *16:* 3286–3294, 1998.
8. Seeger, R. C., Brodeur, G. M., Sather, H., Dalton, A., Siegel, S. E., Wong, K. Y., and Hammond, D. Association of multiple copies of the *N-myc* oncogene with rapid progression of neuroblastomas. N. Engl. J. Med., *313:* 1111–1116, 1985.
9. Schwab, M. Amplification of *N-myc* as a prognostic marker for patients with neuroblastoma. Semin. Cancer Biol., *4:* 13–18, 1993.
10. Cohn, S. L., London, W. B., Huang, D., Katzenstein, H. M., Salwen, H. R., Reinhart, T., Madafiglio, J., Marshall, G. M., Norris, M. D., and Haber, M. *MYCN* expression is not prognostic of adverse outcome in advanced-stage neuroblastoma with nonamplified *MYCN*. J. Clin. Oncol., *18:* 3604–3613, 2000.
11. Dang, C. V., Resar, L. M., Emison, E., Kim, S., Li, Q., Prescott, J. E., Wonsey, D., and Zeller, K. Function of the *c-Myc* oncogenic transcription factor. Exp. Cell Res., *253:* 63–77, 1999.
12. Redolfi, E., Pizzuti, A., Di Bacco, A., Susani, L., Labella, T., Affer, M., Montagna, C., Reinbold, R., Mumm, S., Vezzoni, P., and Zucchi, I. Mapping of the *MYCL2* processed gene to Xq22-23 and identification of an additional *L MYC*-related sequence in Xq27.2. FEBS Lett., *446:* 273–277, 1999.
13. Blackwell, T. K., Kretzner, L., Blackwood, E. M., Eisenman, R. N., and Weintraub, H. Sequence-specific DNA binding by the c-Myc protein. Science (Wash. DC), *250:* 1149–1151, 1990.
14. Ma, A., Moroy, T., Collum, R., Weintraub, H., Alt, F. W., and Blackwell, T. K. DNA binding by N- and L-Myc proteins. Oncogene, *8:* 1093–1098, 1993.
15. Claassen, G. F., and Hann, S. R. *Myc*-mediated transformation: the repression connection. Oncogene, *18:* 2925–2933, 1999.
16. Park, D. S., Razani, B., Lasorella, A., Schreiber-Agus, N., Pestell, R. G., Iavarone, A., and Lisanti, M. P. Evidence that *Myc* isoforms transcriptionally repress caveolin-1 gene expression via an INR-dependent mechanism. Biochemistry, *40:* 3354–3362, 2001.
17. Schwab, M., Varmus, H. E., and Bishop, J. M. Human *N-myc* gene contributes to neoplastic transformation of mammalian cells in culture. Nature (Lond.), *316:* 160–162, 1985.
18. Rupnow, B. A., Murtha, A. D., Chen, E., and Knox, S. J. *Myc* activation reduces fibroblast clonogenicity via an apoptotic mechanism that can be suppressed by a soluble paracrine factor. Cancer Lett., *127:* 211–219, 1998.
19. Yu, Q., He, M., Lee, N. H., and Liu, E. T. Identification of *Myc*-mediated death response pathways by microarray analysis. J. Biol. Chem., *277:* 13059–13066, 2002.
20. Aubry, S., and Charron, J. N-Myc shares cellular functions with *c-Myc*. DNA Cell Biol., *19:* 353–364, 2000.
21. Goodman, L. A., Liu, B. C., Thiele, C. J., Schmidt, M. L., Cohn, S. L., Yamashiro, J. M., Pai, D. S., Ikegaki, N., and Wada, R. K. Modulation of *N-myc* expression alters the invasiveness of neuroblastoma. Clin. Exp. Metastasis, *15:* 130–139, 1997.
22. Weiss, W. A., Aldape, K., Mohapatra, G., Feuerstein, B. G., and Bishop, J. M. Targeted expression of *MYCN* causes neuroblastoma in transgenic mice. EMBO J., *16:* 2985–2995, 1997.
23. Semov, A., Marcotte, R., Semova, N., Ye, X., and Wang, E. Microarray analysis of E-box binding-related gene expression in young and replicatively senescent human fibroblasts. Anal. Biochem., *302:* 38–51, 2002.
24. Shohet, J. M., Hicks, M. J., Plon, S. E., Burlingame, S. M., Stuart, S., Chen, S. Y., Brenner, M. K., and Nuchtern, J. G. Minichromosome maintenance protein MCM7 is a direct target of the *MYCN* transcription factor in neuroblastoma. Cancer Res., *62:* 1123–1128, 2002.
25. Spengler, B. A., Lazarova, D. L., Ross, R. A., and Biedler, J. L. Cell lineage and differentiation state are primary determinants of MYCN gene expression and malignant potential in human neuroblastoma cells. Oncol. Res., *9:* 467–476, 1997.
26. Puga, A., Maier, A., and Medvedovic, M. The transcriptional signature of dioxin in human hepatoma HepG2 cells. Biochem. Pharmacol., *60:* 1129–1142, 2000.
27. Venables, W. N., and Ripley, B. D. Modern Applied Statistics with S-Plus, Ed. 2, pp. 221–222. Heidelberg, Germany: Springer, 1997.
28. Argani, P., Antonescu, C. R., Illei, P. B., Lui, M. Y., Timmons, C. F., Newbury, R., Reuter, V. E., Garvin, A. J., Perez-Atayde, A. R., Fletcher, J. A., Beckwith, J. B., Bridge, J. A., and Ladanyi, M. Primary renal neoplasms with the *ASPL-TFE3* gene fusion of alveolar soft part sarcoma: a distinctive tumor entity previously included among renal cell carcinomas of children and adolescents. Am. J. Pathol., *159:* 179–192, 2001.
29. Goto, S., Umehara, S., Gerbing, R. B., Stram, D. O., Brodeur, G. M., Seeger, R. C., Lukens, J. N., Matthay, K. K., and Shimada, H. Histopathology (International Neuroblastoma Pathology Classification) and *MYCN* status in patients with peripheral neuroblastic tumors: a report from the Children's Cancer Group. Cancer (Phila.), *92:* 2699–2708, 2001.
30. Ahn, J. H., Lee, Y., Jeon, C., Lee, S. J., Lee, B. H., Choi, K. D., and Bae, Y. S. Identification of the genes differentially expressed in human dendritic cell subsets by cDNA subtraction and microarray analysis. Blood, *100:* 1742–1754, 2002.
31. Hiemstra, J. L., Schneider, S. S., and Brodeur, G. M. High-resolution mapping of the *N-myc* amplicon core domain in neuroblastomas. Prog. Clin. Biol. Res., *385:* 51–57, 1994.
32. Nisen, P. D., Waber, P. G., Rich, M. A., Pierce, S., Garvin, J. R. Jr., Gilbert, F., and Lanzkowsky, P. N-Myc oncogene RNA expression in neuroblastoma. J. Natl. Cancer Inst. (Bethesda), *80:* 1633–1637, 1988.
33. Slavc, I., Ellenbogen, R., Jung, W. H., Vawter, G. F., Kretschmar, C., Grier, H., and Korf, B. R. *myc* gene amplification and expression in primary human neuroblastoma. Cancer Res., *50:* 1459–1463, 1990.
34. Chan, H. S., Gallie, B. L., DeBoer, G., Haddad, G., Ikegaki, N., Dimitroulakos, J., Yeger, H., and Ling, V. MYCN protein expression as a predictor of neuroblastoma prognosis. Clin. Cancer Res., *3:* 1699–1706, 1997.
35. Ballestar, E., and Esteller, M. The impact of chromatin in human cancer: linking DNA methylation to gene silencing. Carcinogenesis (Lond.), *23:* 1103–1109, 2002.
36. Shtivelman, E. A link between metastasis and resistance to apoptosis of variant small cell lung carcinoma. Oncogene, *14:* 2167–2173, 1997.
37. Ikura, T., Ogryzko, V. V., Grigoriev, M., Groisman, R., Wang, J., Horikoshi, M., Scully, R., Qin, J., and Nakatani, Y. Involvement of the *TIP60* histone acetylase complex in DNA repair and apoptosis. Cell, *102:* 463–473, 2000.
38. Hirota, S., Isozaki, K., Moriyama, Y., Hashimoto, K., Nishida, T., Ishiguro, S., Kawano, K., Hanada, M., Kurata, A., Takeda, M., Muhammad Tunio, G., Matsuzawa, Y., Kanakura, Y., Shinomura, Y., and Kitamura, Y. Gain-of-function mutations of *c-kit* in human gastrointestinal stromal tumors. Science (Wash. DC), *279:* 577–580, 1998.
39. Lutcke, A. Parton, R. G., Murphy, C., Olkkonen, V. M., Dupree, P., Valencia, A., Simons, K., and Zerialm, M. Cloning and subcellular localization of novel rab proteins reveals polarized and cell type-specific expression. J. Cell Sci., *107:* 3437–3448, 1994.
40. Mavilio, F., Simeone, A., Giampaolo, A., Faiella, A., Zappavigna, V., Acampora, D., Poiana, G., Russo, G., Peschle, C., and Boncinelli, E. Differential and stage-related expression in embryonic tissues of a new human homoeobox gene. Nature (Lond.), *324:* 664–668, 1986.
41. Simeone, A., Mavilio, F., Acampora, D., Giampaolo, A., Faiella, A., Zappavigna, V., D'Esposito, M., Pannese, M., Russo, G., Boncinelli, E., *et al.* Two human homeobox genes, *c1* and *c8*: structure analysis and expression in embryonic development. Proc. Natl. Acad. Sci. USA, *84:* 4914–4918, 1987.
42. Hai, M., Muja, N., DeVries, G. H., Quarles, R. H., and Patel, P. I. Comparative analysis of Schwann cell lines as model systems for myelin gene transcription studies. J. Neurosci. Res., *69:* 497–508, 2002.
43. Taylor, V., and Suter, U. Epithelial membrane protein-2 and epithelial membrane protein-3: two novel members of the peripheral myelin protein 22 gene family. Gene (Amst.), *175:* 115–120, 1996.
44. Gross, N., Balmas, K., and Brognara, C. B. Absence of functional CD44 hyaluronan receptor on human *NMYC*-amplified neuroblastoma cells. Cancer Res., *57:* 1387–1393, 1997.
45. Bujo, H., Hermann, M., Kaderli, M. O., Jacobsen, L., Sugawara, S., Nimpf, J., Yamamoto, T., and Schneider, W. J. Chicken oocyte growth is mediated by an eight ligand binding repeat member of the LDL receptor family. EMBO J., *13:* 5165–5175, 1994.
46. Spiegel, I., Salomon, D., Erne, B., Schaeren-Wiemers, N., and Peles, E. Caspr3 and *caspr4*, two novel members of the *caspr* family are expressed in the nervous system and interact with *PDZ* domains. Mol. Cell. Neurosci., *20:* 283–297, 2002.
47. Nagase, T., Ishikawa, K., Suyama, M., Kikuno, R., Miyajima, N., Tanaka, A., Kotani, H., Nomura, N., and Ohara, O. Prediction of the coding sequences of unidentified human genes. XI. The complete sequences of 100 new cDNA clones from brain which code for large proteins *in vitro*. DNA Res., *5:* 277–286, 1998.
48. Ackerman, S. L., and Knowles, B. B. Cloning and mapping of the *UNC5C* gene to human chromosome 4q21–q23. Genomics, *52:* 205–208, 1998.
49. Prescott, J. E., Osthus, R. C., Lee, L. A., Lewis, B. C., Shim, H., Barrett, J. F., Guo, Q., Hawkins, A. L., Griffin, C. A., and Dang, C. V. A novel *c-Myc*-responsive gene, JPO1, participates in neoplastic transformation. J. Biol. Chem., *276:* 48276–48284, 2001.
50. Berwanger, B., Hartmann, O., Bergmann, E., Bernard, S., Nielsen, D., Krause, M., Kartal, A., Flynn, D., Wiedemeyer, R., Schwab, M., Schafer, H., Christiansen, H., and Eilers, M. Loss of a *FYN*-regulated differentiation and growth arrest pathway in advanced stage neuroblastoma. Cancer Cell, *2:* 377–386, 2002.
51. Cornelis, S., Bruynooghe, Y., Denecker, G., Van Huffel, S., Tinton, S., and Beyaert, R. Identification and characterization of a novel cell cycle-regulated internal ribosome entry site. Mol. Cell, *5:* 597–605, 2000.
52. Caron, H., van Sluis, P., van Hoeve, M., de Kraker, J., Bras, J., Slater, R., Mannens, M., Voute, P. A., Westerveld, A., and Versteeg, R. Allelic loss of chromosome 1p36 in neuroblastoma is of preferential maternal origin and correlates with *N-myc* amplication. Nat. Genet., *4:* 187–190, 1993.
53. Lahti, J. M., Valentine, M., Xiang, J., Jones, B., Amann, J., Grenet, J., Richmond, G., Look, A. T., and Kidd, V. J. Alterations in the PITSLRE protein kinase gene complex on chromosome 1p36 in childhood neuroblastoma. Nat. Genet., *7:* 370–375, 1994.
54. Hirose, T., Tamaru, T., Okumura, N., Nagai, K., and Okada, M. PCTAIRE 2, a Cdc2-related serine/threonine kinase, is predominantly expressed in terminally differentiated neurons. Eur. J. Biochem., *249:* 481–488, 1997.

55. Shen, Z., Pardington-Purtymun, P. E., Comeaux, J. C., Moyzis, R. K., and Chen, D. J. UBL1, a human ubiquitin-like protein associating with human RAD51/RAD52 proteins. Genomics, *36:* 271–279, 1996.
56. Li, W., Hesabi, B., Babbo, A., Pacione, C., Liu, J., Chen, D. J., Nickoloff, J. A., and Shen, Z. Regulation of double-strand break-induced mammalian homologous recombination by UBL1, a RAD51-interacting protein. Nucleic Acids Res., *28:* 1145–1153, 2000.
57. Fujioka, Y., Kimata, Y., Nomaguchi, K., Watanabe, K., and Kohno, K. Identification of a novel non-structural maintenance of chromosomes (*SMC*) component of the *SMC5-SMC6* complex involved in DNA repair. J. Biol. Chem., *277:* 21585–21591, 2002.
58. Wang, C. X., Wadehra, M., Fisk, B. C., Goodglick, L., and Braun, J. Epithelial membrane protein 2, a 4-transmembrane protein that suppresses B-cell lymphoma tumorigenicity. Blood, *97:* 3890–3895, 2001.
59. Walter, L., Marynen, P., Szpirer, J., Levan, G., and Gunther, E. Identification of a novel conserved human gene, TEGT. Genomics, *28:* 301–304, 1995.
60. Ejeskar, K., Abel, F., Sjoberg, R., Backstrom, J., Kogner, P., and Martinsson, T. Fine mapping of the human preprocortistatin gene (*CORT*) to neuroblastoma consensus deletion region 1p36.3→p36.2, but absence of mutations in primary tumors. Cytogenet. Cell Genet., *89:* 62–66, 2000.
61. Boon, K., Caron, H. N., van Asperen, R., Valentijn, L., Hermus, M. C., van Sluis, P., Roobeek, I., Weis, I., Voute, P. A., Schwab, M., and Versteeg, R. N-Myc enhances the expression of a large set of genes functioning in ribosome biogenesis and protein synthesis. EMBO J., *20:* 1383–1393, 2001.
62. Godfried, M. B., Veenstra, M., v Sluis, P., Boon, K., v Asperen, R., Hermus, M. C., v Schaik, B. D., Voute, T. P., Schwab, M., Versteeg, R., and Caron, H. N. The *N-myc* and *c-myc* downstream pathways include the chromosome 17q genes *nm23–H1* and *nm23–H2*. Oncogene, *21:* 2097–2101, 2002.